Biocomputational analysis of phosphoenolpyruvate carboxykinase from *Raillietina echinobothrida*, a cestode parasite, and its interaction with possible modulators

ASIM KUMAR DUTTA, RAMNATH, VEENA TANDON *and* BIDYADHAR DAS*

Department of Zoology, North-Eastern Hill University, Shillong, Meghalaya-793022, India

(*Received 4 June 2015; revised 23 November 2015; accepted 23 November 2015; first published online 22 December 2015*)

SUMMARY

Phosphoenolpyruvate carboxykinase (PEPCK) involved in gluconeogenesis in higher vertebrates opposedly plays a significant role in glucose oxidation of the cestode parasite, *Raillietina echinobothrida*. Considering the importance of the enzyme in the parasite and lack of its structural details, there exists an urgent need for understanding the molecular details and development of possible modulators. Hence, in this study, PEPCK gene was obtained using rapid amplification of cDNA ends, and various biocomputational analyses were performed. Homology model of the enzyme was generated, and docking simulations were executed with its substrate, co-factor, and modulators. Computer hits were generated after structure- and ligand-based screening using Discovery Studio 4.1 software; the predicted interactions were compared with those of the existing structural information of PEPCK. In order to evaluate the docking simulation results of the modulators, PEPCK gene was cloned and the overexpressed protein was purified for kinetic studies. Enzyme kinetics and *in vitro* studies revealed that out of the modulators tested, tetrahydropalmatine (THP) inhibited the enzyme with lowest inhibition constant value of 93 nM. Taking the results together, we conclude that THP could be a potential inhibitor for PEPCK in the parasite.

Key words: Cestode, PEPCK (GTP), molecular docking, THP, enzyme kinetics.

INTRODUCTION

Phosphoenolpyruvate carboxykinase (PEPCK, EC 4.1.1.32) catalyses the metabolic reversible reaction, i.e. formation of phosphoenolpyruvate (PEP) from oxaloacetic acid (OAA), in higher organisms. This enzyme is reported to be metabolically involved in gluconeogenesis, glyceroneogenesis, synthesis of serine and conversion of amino acids, such as glutamine and glutamate, to PEP (Yang *et al*. 2009). PEPCK uses GTP or ITP (ATP in bacteria and yeast) and metal ions for its activity. In contrast, in cestode parasites, including *Raillietina echinobothrida* (Platyhelminthes: Cestoda; Cyclophyllidea), PEPCK catalyses the carboxylation step, i.e. formation of OAA from PEP, in glucose oxidation (Smyth and McManus, 1989; Tandon and Das, 2007). Cestode parasites mainly depend on carbohydrates for their energy derivation, and have limited ability to metabolize lipids and proteins (Smyth and McManus, 1989). Hence, the role of PEPCK in glucose oxidation in these parasites is highlighted, and inhibiton of the enzyme might down regulate the utilization of carbohydrates. Because of the differing primary function of PEPCK in cestodes and their vertebrate hosts, this step of glucose oxidation is regarded as a plausible anthelmintic target (Reynolds, 1980).

Reported for the first time in chicken liver among vertebrates (Utter and Kurahashi, 1954), PEPCK is present in two forms, cytosolic and mitochondrial, in higher vertebrates (Jo *et al*. 1974). cDNA sequences of PEPCK (both isoforms) from the avian host, *Gallus gallus*, have been deduced (Cook *et al*. 1986; Weldon *et al*. 1990). However, the knowledge of molecular details of this enzyme is limited to only few helminths, e.g. *Schistosoma japonicum* (Liu *et al*. 2006), *Clonorchis sinensis* (Wang *et al*. 2011), *Taenia asiatica* (Knapp *et al*. 2011), *Haemonchus contortus* (Klein *et al*. 1992), *Ascaris suum* (Rios and Nowak, 2002), and *Brugia malayi* (Ghedin *et al*. 2007). From previous reports, it has been seen that genistein and its derivatives alters the activity of PEPCK in *R. echinobothrida* when treated *in vitro* (Das *et al*. 2004). Recently, PEPCK from the parasite was purified biochemically and characterized (Das *et al*. 2013). However, molecular and structural details of the enzyme are not known so far. Structural analysis of PEPCK provides a detailed mechanism of the enzyme reaction and its regulation (Holyoak, *et al*. 2006). Virtual screening along with molecular modelling and docking help to design active novel enzyme inhibitors and pharmacophores (Rollinger *et al*. 2008). Since the mRNA sequence of PEPCK from the parasite is unavailable, *in silico* studies, motifs/domains, three-dimensional structure

* Corresponding author: Biological Chemistry Laboratory, Department of Zoology, North-Eastern Hill University, Shillong-793022, Meghalaya, India. E-mail: dasbidyadhar@gmail.com

Parasitology (2016), **143**, 300–313.
doi:10.1017/S0031182015001742

and functional studies of the enzyme in *R. echinobothrida* are largely unknown. To evaluate and understand the molecular details of the enzyme from the cestode parasite, the present study was undertaken. For this purpose, the coding DNA sequence (CDS) encoding PEPCK gene was obtained using rapid amplification of cDNA ends (RACE), and analysed using various *in silico* tools. The homology modelling of PEPCK was undertaken and the resultant model was subjected to molecular docking analyses with substrate and co-factor. A few possible modulators were also docked into the active site of the enzyme in order to analyse their interactions. The analyses of *in silico* results were validated using enzyme kinetics and *in vitro* study, and discussed in the light of available data accessed from crystallographic studies of PEPCK.

MATERIALS AND METHODS

Vectors and chemicals

pGEM-T easy cloning vector (Code no. A1360) was procured from Promega, USA, and Purelink RNA isolation kit (Code no. 12183018A) and SuperScript III first strand reverse transcriptase-polymerase chain reaction (RT-PCR) reaction kit (Code no. 18080051) were from Invitrogen, USA, whereas SMARTer™ RACE cDNA amplification kit (Code no. 634923) was from Takara Clontech, USA. GenElute gel extraction kit (Code no. NA1111) was obtained from Sigma, USA. Restriction enzymes and other enzymes were procured from New England Biolabs Ltd. (UK). Other reagents and chemicals, supplied either from Sigma, USA, or Sisco Research Laboratories (SRL), India, were of the highest analytical grade.

The parasite and total RNA isolation

The parasite, *R. echinobothrida*, was collected from the small intestine of chicken, and morphologically identified by the presence of a heavily armed rostellum with two rows of hooklets and four circular suckers on the scolex (Soulsby, 1982). Immediately, total RNA was isolated from the parasite using Purelink RNA mini kit following manufacturers' protocol. RNA was then quantified using Nanodrop 2000 (Thermo Scientific) and its integrity was checked on 1·2% agarose gel.

RACE and cloning

About 2 μg of total RNA from *R. echinobothrida* was taken, and the first strand synthesis was performed by using the Super Script III first strand RT-PCR reaction kit following manufacturers' protocol. All the relevant primers used in RACE and cloning of PEPCK are given in online supplementary Table 1. RT-PCR was performed using degenerate primers from the conserved regions against the cDNA sequence of *Taenia solium* (GenBank acc. no. FN567996.1). The PCR product was gel eluted using GenElute gel extraction kit, purified and sequenced. PEPCK amino acid sequences from different species were aligned against the translated sequence (partial CDS) using Clustal Omega (http://www.ebi.ac.uk/Tools/msa/clustalo); and gene specific primers were designed from the conserved regions against the partial CDS of PEPCK.

5′- and 3′-RACE were performed using the partial CDS of PEPCK following SMARTer™ RACE cDNA amplification kit protocol. The 5′-RACE-PCR reaction was carried out using PCK and 5′-RACE outer primer. Nested PCR was performed using PCK along with 5′-RACE inner primer by using primary PCR product as template. PCR reactions were carried out using the following parameters: initial denaturation of 94 °C for 5 min, followed by 30 cycles of denaturation (94 °C for 30 s), annealing (65 °C for 60 s) and primer extension (72 °C for 2 min), followed by final extension step (72 °C for 10 min). Similar procedure and thermal conditions were followed to carry out 3′-RACE-PCR, in which PCK and 3′-RACE outer and PCK and 3′-RACE inner primers were used for the initial and nested PCR reactions, respectively. Amplified DNA fragments of both 5′- and 3′-RACE were cloned into pGEM-T easy cloning vector, transformed into *Escherichia coli* (DH5α) competent cells, and plated onto the Luria-Bertani (LB) agar plate containing 100 μg mL^{-1} ampicillin. Positive clones were selected and plasmids were isolated and sequenced. Sequences of core fragment, 5′- and 3′-RACE products were assembled by NCBI *vs* NCBI/BLAST/blastn suite (https://blast.ncbi.nlm.nih.gov/Blast.cgi), and full length cDNA sequence of PEPCK gene was obtained. NCBI BLAST was used for the GenBank search and similarity assessment. The ORF of PEPCK was then amplified using LD_PCK_FP and LD_PCK_RP primers and cloned into pGEM-T easy vector.

Sequence analysis

The complete CDS of PEPCK from the parasite was conceptually translated using ExPASy-Translate tool (http://web.expasy.org/cgi-bin/translate/dna). PEPCK amino acid sequences of *T. asiatica* (CBH36498.1), *A. suum* (ADY43130.1), *H. contortus* (AAA29180.1), *Caenorhabditis elegans* (CAF31482.1), *S. japonicum* (AAW25103.1), *Schistosoma mansoni* (AAD24794.1), and cytosolic and mitochondrial isoforms of *G. gallus* (NP_990802.1 and NP_990801.1), *Rattus norvegicus* (NP_942075.1 and NP_001101847.2), and *Homo sapiens* (NP_002582.3 and EAW66115.1) were accessed from NCBI Protein database (http://www.ncbi.nlm.nih.gov/protein). Multiple

https://doi.org/10.1017/S0031182015001742 Published online by Cambridge University Press

sequence alignment was carried out to assess the degree of homology and consensus sequences using Clustal Omega.

The properties of the enzyme (number of amino acids, molecular weight, theoretical pI, secondary structures, phosphorylation sites, disulphide bonds and O-linked β-N-acetylglucosamine sites (O-GlcNAc)) were determined and compared with other related species using ExPASy – ProtParam tool (http://web.expasy.org/protparam/), Discovery Studio 4.1 software (Accelrys-Biovia) (DS 4.1), NetPhos 2.0 server (http://www.cbs.dtu.dk/services/NetPhos/), DISULFIND (http://disulfind.dsi.unifi.it/), and CBS prediction servers (http://genome.cbs.dtu.dk). Default parameters were used during *in silico* analyses, unless specified otherwise.

Homology modelling

Homology model of *R. echinobothrida* PEPCK containing PEP-GDP-2Mn^{2+} was prepared using DS 4.1. The crystal structure of rat cytosolic PEPCK-PEP-GDP complex (PDB ID 4GNP) served as structural reference. The template was aligned with the target sequence and examined for conserved sequences. The query and template proteins belong to the same family and class as defined by 'Structural Classification of Proteins'. The ligands found in the template structure (GDP^{701}, Mn^{702}, PEP^{703}, and Mn^{705}) were incorporated into PEPCK model. DS 4.1 was used to build 1000 homology models for the query sequence, and best model was selected based on the lowest probability density functions (PDF) energy, discrete optimized protein energy (DOPE) score and root mean square deviation (RMSD) value. Side chain refinement was done using chi-rotor algorithm, and the generated refined model was used for docking studies. The model was then verified in the software, which resulted in a verify score, higher than the expected high score, suggesting it to be a good model. The model was also validated using Volume, Area, Dihedral Angle Reporter (VADAR) program (http://vadar.wishartlab.com). For *in silico* comparison of the structure and interaction studies between the parasite- and host-PEPCK, the available crystal structure of mitochondrial chicken PEPCK (PDB ID 2FAF) was used. In order to check whether other online bioinformatics tools result in similar structure or not, a model was also built using SWISS-MODEL tool (http://swissmodel.expasy.org) using the same template (PDB ID 4GNP). The models generated from both sources were structurally aligned to find out difference in their catalytic regions, if any. Active site residues of the prepared model were manually checked with both the template and the available crystal structure of chicken mitochondrial PEPCK (PDB ID 2FAF).

Molecular docking

The model was further refined using 'Macromolecules (Prepare protein)' tool of DS 4.1. During refinement, water molecules were removed, missing hydrogen atoms were added and then the receptor molecules were optimized by energy minimization till the root mean square gradient reached about 0·2–0·4. The energy-minimized receptor molecule was used for molecular docking. The domains and active site residues of PEPCK were analysed from NCBI conserved domain search (www.ncbi.nlm.nih.gov/Structure/cdd/cddsrv.cgi) and CASTp server (www.sts.bioe.uic.edu/castp). In the case of docking of the modulators, the binding sites were defined from receptor cavities having the largest binding site volume using 'Define and edit binding' tool (DS 4.1).

Molecular docking was performed with the selected ligands against the modelled PEPCK by using DS 4.1 CDocker. The ligands were docked into the binding site of PEPCK by selecting the pocket (sphere) of the receptor molecules. The energy-minimized complex was loaded in the workspace of DS 4.1. After docking the ligands into the receptor, the top scoring molecules were considered for further evaluation. The best pose for each docked molecule was selected by analysing binding efficiency, binding energy, hydrogen bonds, non-bonded interactions, and the most populated cluster. Binding energies (CDocker energy) were calculated by typing the docked molecules with Chemistry at HARvard Macromolecular Mechanics (CHARMm) forcefield method using 'Dock ligands' (Scoring-Calculate binding energies) tool of DS 4.1.

As reviewed from the literature, possible modulators for PEPCK, e.g. tetrahydropalmitine (THP, CID 72301), genistein (CID 5280961), praziquantel (PZQ, CID 4891) and daidzein (CID 5281708), were retrieved from PubChem database (https://pubchem.ncbi.nlm.nih.gov) in canonical simplified molecular input line entry system (SMILES) format, hydrogen atoms were added, and then optimized by using 'Small molecules' (Prepare ligand) tool of DS 4.1. These modulators were docked into the predicted active site of PEPCK. The predicted interactions and binding affinities of these molecules for PEPCK were determined following the procedure mentioned above.

Cloning, expression and purification of PEPCK

In order to validate the docking simulation results, the effect of possible modulators was tested on kinetics of PEPCK. In brief, the ORF of PEPCK was sub-cloned into pE-SUMO expression vector (kindly provided by Dr. Todd Holyoak, University of Waterloo, Canada) using the primers

https://doi.org/10.1017/S0031182015001742 Published online by Cambridge University Press

pE_PCK_FP having BsmB1 cut site and pE_PCK_RP having Xho1 cut site. The construct was then transformed into *E. coli* BL21, induced by Isopropyl β-D-1-thiogalactopyranoside (IPTG) (1 mM) overnight at 20 °C. The recombinant His-tagged PEPCK was purified using Ni-NTA agarose (Ni^{2+}-nitrilotriacetate agarose), and protein was eluted at 300 mM imidazole. The N-terminal fusion was cleaved by SUMO protease (1 U μL^{-1}) overnight at 4 °C, and the purified PEPCK was used for enzyme kinetics.

Enzyme kinetics and inhibitory constant (Ki) of modulators

Kinetics of the recombinant PEPCK in the direction of PEP carboxylation was assayed spectrophotometrically (Cary 60 UV-Vis, Agilent Technologies, USA) at 40 °C according to the modified method of Mommsen *et al*. (1985). In brief, 1·0 mL reaction mixture contained 50 mM Tris-HCl buffer (pH 7·4), 5 mM PEP, 0·2 mM NADH, 0·6 mM GDP, 20 mM $NaHCO_3$, 4 mM $MnCl_2$ and 10 units of MDH. The reaction mixture was pre-incubated for 5 min and an appropriately diluted enzyme was added to initiate the reaction. The background and negative controls were maintained without NADH and the enzyme, respectively. The enzyme activity was calculated by taking $6{\cdot}22 \times 10^6$ as the molar extinction co-efficient for NADH. One unit (U) of enzyme activity is defined as the amount of the enzyme that catalyses oxidation of 1 μmole of NADH per min under standard assay conditions. Protein concentration was determined using Bradford's reagent (Bradford, 1976) and bovine serum albumin was used as the standard. Specific activity was expressed as U mg^{-1} of protein.

Three different concentrations (5, 10 and 20 μM) of each modulator were studied in presence of variable concentrations of the substrate (0·01–8 mM). Inhibitory constant (*K*i) for the modulators was calculated by plotting the reaction rates at varying concentrations of the substrate (Michaelis–Menten and Lineweaver–Burk plots).

Treatment of parasites and PEPCK activity

In order to find out their biological significance, the modulators (THP, genistein, PZQ and daidzein) were tested on the parasite *in vitro*. Onset of paralysis, absence of motility upon physical disturbance, in the parasites was also recorded by visually examining them every 15 min. For enzyme kinetic studies, for each set of experiment, 3 numbers of live parasites (about 0·2 g wet wt.) with roughly same size and developmental stage were incubated at 40 °C in 10 mL of PBS (pH 7·4) containing 5 mM D-glucose and 1 mM of respective modulator dissolved in DMSO along with simultaneous maintenance of control, with and without the vehicle (DMSO with maximum concentration of 1%). After 4 h of treatment (2 h in the case of PZQ), the parasites were collected and snap-frozen, and processed for enzyme activity. A 10% (w/v) homogenate was made, within 24 h, from the snap-frozen parasites in Tris-HCl homogenate buffer (50 mM, pH 7·4) containing 0·25 M sucrose, 2 mM EDTA, 1 mM DTT and 0·01 mM PMSF. The homogenate was treated with 1·0 volume of 0·5% Triton X-100 for 30 min, and sonicated for 10 cycles (30 s pulse at 25 W with 30 s interval) at 4 °C using a sonicator (Soniprep 150). The homogenate was then spun at 10 000 g for 30 min, and the resultant supernatant was used for enzyme kinetics. All steps were carried out at 4 °C. PEPCK activity was assayed spectrophotometrically in the direction of PEP carboxylation following the method as mentioned in the preceding section above.

Dosage- and time-dependent experiments were also performed in order to find out the effect of THP and genistein on PEPCK activity in the parasite.

Statistical analysis

In this study, all experimental data were presented as the mean ± S.E.M. ($n = 4$). Probability value $<0{\cdot}05$ was considered as statistically significant. Co-efficient of bivariate regression line was calculated using OriginPro 8 software and the co-efficient for linear lines was $\geqslant 0{\cdot}9$ ($R^2 \geqslant 0{\cdot}9$).

RESULTS

RACE and analysis of PEPCK sequence

A core amplicon of 627 bp was obtained using degenerate primers, and 5′- and 3′-RACE were carried out in order to get the complete CDS of PEPCK. The complete CDS of 2166 bp (online supplementary Fig. 1) was obtained and submitted to NCBI (GenBank acc. no. KC252609.1), which contained an ORF of 1884 bp, starting with an 'ATG' codon at position 32 and ending with the stop codon 'TAA' at position 1918, with 5′- and 3′-untranslated region (UTR) of 31 bp and 248 bp, respectively (online supplementary Fig. 2). Clustal Omega analysis of the sequence revealed various conserved domains; R-loop (^{88}VARVESKT^{95}) and PEPCK-specific domain (^{238}GSGYGGNSLLGKK^{250}) for substrate binding, kinase-1 motif or P-loop domain (^{290}FPSACGKT^{297}) for nucleotide binding, kinase-2 motif (^{313}CVGDD^{317}) for metal binding, and the mobile Ω-loop catalytic domain (^{470}SEATAAAEFKGRQVM^{484}) involved in enzyme catalysis (Fig. 1).

PEPCK encoded a protein of 628 amino acids having a theoretical molecular mass of 70·9 kDa, and a predicted pI of 7·57 (Table 1). The aliphatic,

https://doi.org/10.1017/S0031182015001742 Published online by Cambridge University Press

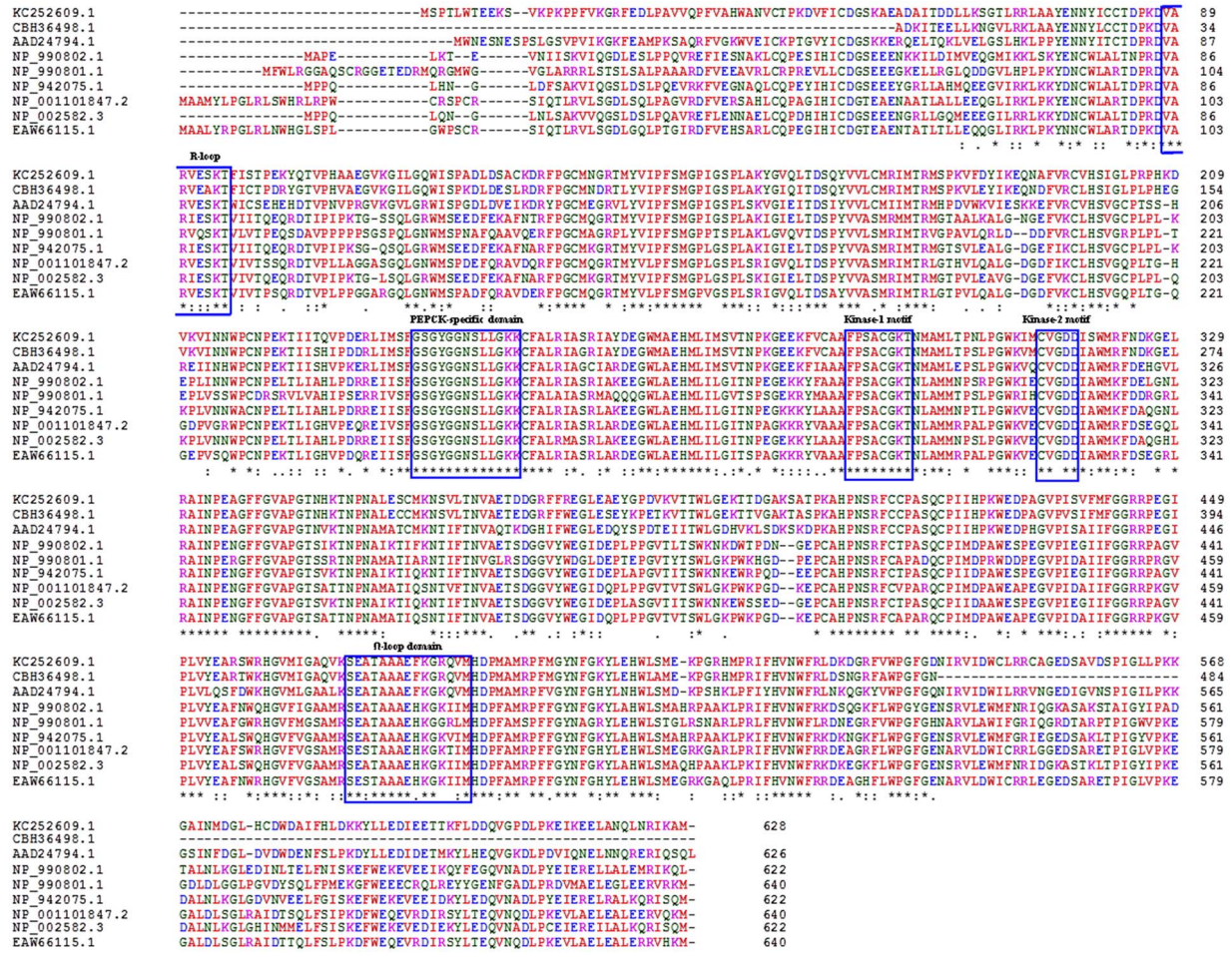

Fig. 1. Alignment of amino acid sequences of PEPCK. Amino acid sequences of the enzyme were accessed from NCBI database: KC252609.1 (*R. echinobothrida*), CBH36498.1 (*T. asiatica*), AAD24794.1 (*S. mansoni*), NP_990802.1 (*G. gallus* (cytosolic)), NP_990801.1 (*G. gallus* (mitochondrial)), NP_942075.1 (*R. norvegicus* (cytosolic)), NP_001101847.2 (*R. norvegicus* (mitochondrial)), NP_002582.3 (*H. sapiens* (cytosolic)), and EAW66115.1 (*H. sapiens* (mitochondrial)). The putative functional sites are shown in boxes. '*' identical amino acid residues, ':' conserved residues, '.' semi-conserved residues and '–' absence of amino acid in the sequence. Abbreviation: PEPCK, phosphoenolpyruvate carboxykinase.

Table 1. Comparative biochemical analysis of PEPCKs from *R. echinobothrida*, other helminths*, *Xenopus tropicalis*, *G. gallus*, *R. norvegicus* and *H. sapiens* origin. [(c) denotes cytosolic; and (m) denotes mitochondrial]

Species name	GenBank acc. no.	No. of amino acids	Molecular mass (kDa)	Predicted pI
R. echinobothrida	KC252609.1	628	70·9	7·57
Taenia asiatica(partial)*	CBH36498	484	54·1	8·49
*Hymenolepis microstoma**	CDS27807.1	624	69·7	7·43
*Schistosoma japonicum**	AAW25103	626	70·3	6·35
*S. mansoni**	AAD24794	626	70·5	6·75
*Clonorchis sinensis**	GAA49544	800	90·5	8·49
*Ascaris suum**	ADY43130	656	73·4	5·69
*Haemonchus contortus**	AAA29180	619	69·7	6·86
*Caenorhabditis elegans**	CAF31482	587	66·0	5·62
*Brugia malayi**	XP_001896498	691	77·8	5·76
X. tropicalis(c)	AAI24063	604	66·6	6·84
X. tropicalis(m)	CAJ83705	604	66·6	6·84
G. gallus(c)	NP_990802.1	622	69·5	6·10
G. gallus(m)	NP_990801.1	640	71·0	8·16
R. norvegicus(c)	NP_942075	622	69·4	6·09
R. norvegicus(m)	NP_001101847	640	70·7	7·88
H. sapiens(c)	NP_002582	622	69·2	5·80
H. sapiens(m)	EAW66115	640	70·7	7·57

PEPCK, phosphoenolpyruvate carboxykinase.

https://doi.org/10.1017/S0031182015001742 Published online by Cambridge University Press

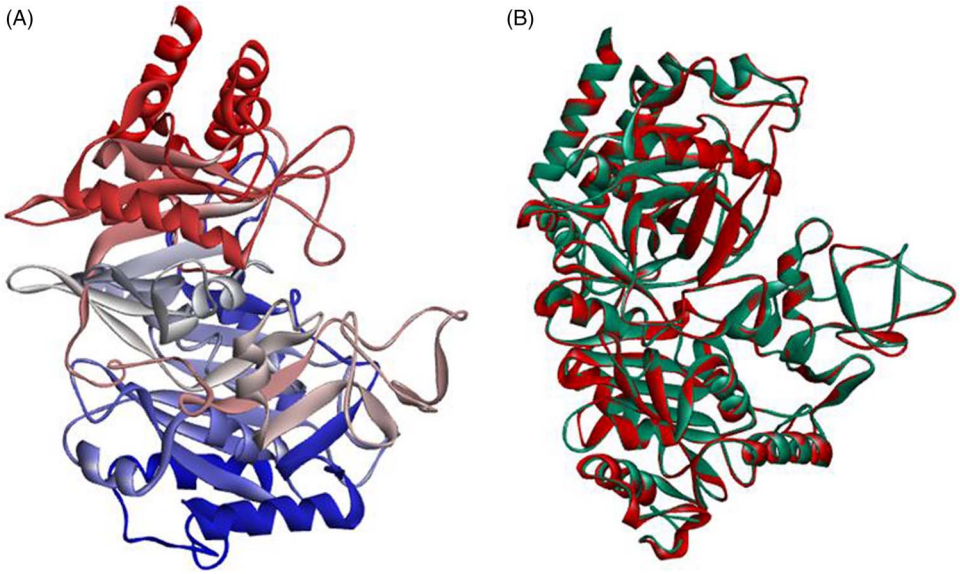

Fig. 2. Homology model of *R. echinobothrida* PEPCK and its validation. (A) The model (ribbon diagram) was prepared using the crystal structure of rat cytosolic PEPCK Ld_3 g in complex with PEP and GDP (PDB ID 4GNP) as template. N- and C- terminal domains of PEPCK are shown in red and blue colours, respectively. (B) Structural superimposition of the modelled PEPCK from the parasite (in green colour) with its template (red colour) showing a RMSD value of 0·22 Å. Abbreviations: GDP, guanosine diphosphate; PEP, phosphoenolpyruvate; PEPCK, phosphoenolpyruvate carboxykinase; RMSD, root mean square deviation.

instability and grand average of hydropathy (GRAVY) indices of PEPCK were calculated and found to be 71·91, 38·95 and −0·313, respectively. The secondary structure, phosphorylation sites, disulphide bonds, and O-GlcNAc sites of PEPCK were also predicted (online supplementary Fig. 3). The secondary structure contained 485 α-helices, 205 β-strands, and 87 turns. Phosphorylation sites of PEPCK were predicted to be S181, S457, T42, and Y103. Amino acids, such as aspartic acid, methionine and cysteine, were found to be more; whereas, glutamine, leucine and serine were less in the parasite PEPCK in comparison with its host counterpart.

Homology modelling and validation of the model

The modelled structure for the PEPCK-PEP-GDP-$2Mn^{2+}$ complex has been shown in Fig. 2A, which has sequence identity of 54·5% and a sequence alignment length of 610 residues with the template (rat cytosolic PEPCK-GDP-PEP-$2Mn^{2+}$ complex, PDB ID 4GNP). The sequence had a fair identity with the template with respect to domains and active sites of the enzyme.

To validate the model, it was superimposed upon the template and the RMSD value was found to be 0·22 Å (Fig. 2B). The PDF energy of PEPCK model was checked, and DOPE score found to be −84 956·65. Ramachandran plot of the model also showed that 96·6% residues were in the most favourable region (online supplementary Fig. 4A). To support these, hydrophobicity plot of the model and the template was investigated and fairly consistent profiles were observed demonstrating that the model was reasonable and could be employed for docking studies (online supplementary Fig. 4B–C). The model was also validated using VADAR program and compared with its structural reference (online supplementary Table 2). The RMSD value between the models, obtained from SWISS-MODEL and DS 4.1, was found to be 0·75 Å, confirming its structural similarity (online supplementary Fig. 5A). This model was also superimposed with crystal structure of its host counterpart (PDB ID 2FAF) showing an RMSD value of 1·05 Å (online supplementary Fig. 5B). Hence, the model generated using DS 4.1 was used for molecular docking studies.

Molecular docking of the substrate, co-factor and modulators

Residues of the conserved domains were selected to form the binding site sphere in DS 4.1. The likely interactions of the substrate and co-factors with various residues of PEPCK model were visualized, and atomic co-ordinates were compared with its structural reference (PDB ID 4GNP) and were found to be similar (Table 2). The modelled PEPCK contained all the catalytic domains; however, due to sequence alignment, the residues positions were different from the original parasite PEPCK sequence. The predicted docking results showed that most of the compounds formed hydrogen bonds with the predicted interacting residues of

https://doi.org/10.1017/S0031182015001742 Published online by Cambridge University Press

Table 2. Comparative analysis of atomic co-ordinates of substrate and cofactors with rat cytosolic PEPCK Ld_3g in complex with PEP and GDP (PDB ID 4GNP) and PEPCK model (in complex with PEP and GDP) of the cestode parasite, *R. echinobothrida*

PEPCK complex	Ligands	Interacting amino acids	Types of bonds	Distance between the atoms (Å)	PEPCK complex	Ligands	Predicted interacting amino acids	Types of bonds	Distance between the atoms (Å)
Rat cytosolic PEPCK Ld_3g in complex with PEP and GDP	GDP	A287	Hydrogen (N–O1B)	2·8	PEPCK model in complex with PEP and GDP	GDP	A293	Hydrogen (N–O1B)	2·82
		G289	Hydrogen (N–O3B)	3			G295	Hydrogen (N–O3B)	3·01
		K290	Hydrogen (N–O3B)	2·8			K296	Hydrogen (N–O3B)	2·82
		T291	Hydrogen (N–O2B)	2·9			T297	Hydrogen (N–O2A)	2·93
			Hydrogen (OG1–O2B)	3				Hydrogen (N–O2B)	3·32
		N292	Hydrogen (N–O2A)	2·8			N298	Hydrogen (N–O2A)	2·79
			Hydrogen (ND2–O2A)	3				Hydrogen (ND2–O2A)	3·06
		R436	Hydrogen (NH1–O4)	3			–	–	–
		F530	Hydrogen (N–O6)	3			F537	Hydrogen (N–O6)	2·96
		N533	Hydrogen (ND2–O6)	3			N540	Hydrogen (N–O6)	3·07
	PEP	R87	Hydrogen (N–O2)	2·9		PEP	R90	Hydrogen (N–O2)	2·9
			Hydrogen (NE–O3P)	2·9				–	
		G237	Hydrogen (N–O1)	2·7			G243	Hydrogen (N–O1)	2·83
		N403	Hydrogen (ND2–O2)	2·9			N411	Hydrogen (ND2–O2)	2·84
		R405	Hydrogen (NH1–O1P)	3·2			R413	Hydrogen (NH1–O1P)	4·46
			Hydrogen (NH2–O1P)	2·9				Hydrogen (NH2–O1P)	2·78
	Mn (1)	H264	Metal interaction (NE2)	2·3		Mn (1)	H270	Metal interaction (NE2)	4·48
		D311	Metal interaction (OD1)	2·2			D317	Metal interaction (O)	2·76
			Metal interaction (OD2)	3·3				–	–
		K244	Metal interaction (NZ)	2·3			K250	Metal interaction (NZ)	2·27
	Mn (2)	T291	Metal interaction (OG1)	2·4		Mn (2)	T297	Metal interaction (O)	2·93

GDP, guanosine diphosphate; Mn, manganese; PEP, phosphoenolpyruvate; PEPCK, phosphoenolpyruvate carboxykinase.

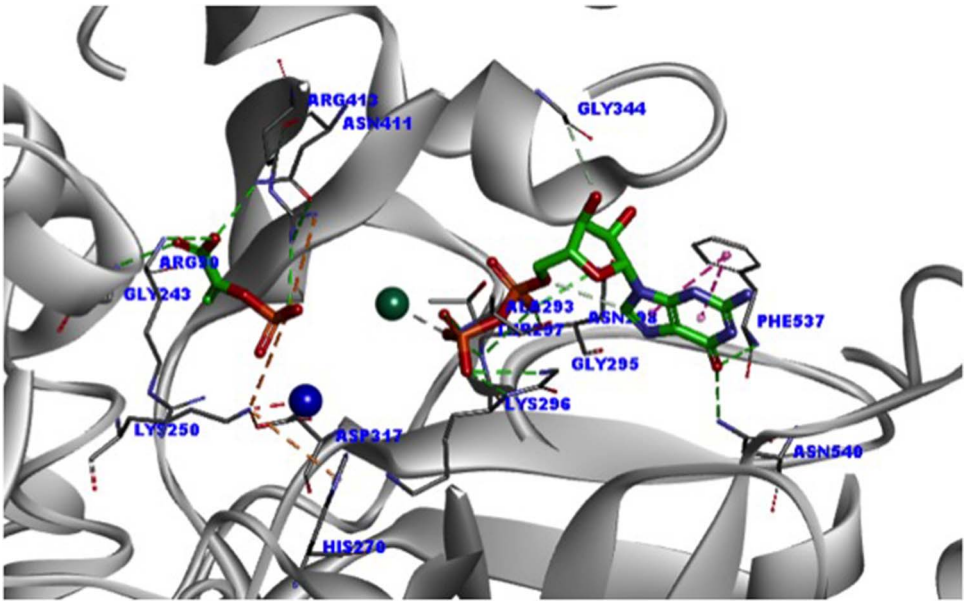

Fig. 3. Homology model of *R. echinobothrida* PEPCK-PEP-GDP-2Mn^{2+} complex. The protein backbone is rendered as a grey ribbon, and dotted lines represent the predicted hydrogen bonds. All catalytic residues are rendered as thin stick models and ligands, as thick stick models. N atoms are in blue colour, O atoms in red, and C atoms in green. First manganese metal ion (M1) is shown in blue CPK model and second manganese metal ion (M2) is shown in green colour. Abbreviations: GDP, guanosine diphosphate; Mn, manganese; PEP, phosphoenolpyruvate; PEPCK, phosphoenolpyruvate carboxykinase.

the modelled PEPCK. The substrate, PEP, was predicted to interact with R90 (R-loop), G243, N411 and R413; and the first metal ion (M1) was found to directly co-ordinate with K250, H270 and D317 residues (Fig. 3). The likely interactions of GDP were observed with A293, G295, K296, T297, N298, F537 and N540 (Fig. 3). In order to validate the accuracy of the co-ordination geometries of the ligands, the docked poses were superimposed with available crystal structure complexes (PDB IDs 4GNP and 4GMW) showing RMSD value of 0·22 and 0·36 Å, respectively (online supplementary Table 3).

The modulators were docked into the modelled PEPCK-PEP-2Mn^{2+} complex. Determination of the probable binding conformation and interactions of modulators showed that THP had similar interactions as seen in the case of GDP (Fig. 4). Analysis of the THP-PEPCK complex revealed that in its most likely binding pose, the ligand behaved as a π-bond donor to A293 and F537, whereas the hydrogen atoms of the ligand served as hydrogen bond acceptors from F537, N540. A non-classical hydrogen bond was also predicted with N540 residue. The ligand was also predicted to occupy a groove and made hydrophobic interactions (π-alkyl) with A293 and F537. In order to examine the difference in affinity of THP, if any, towards the enzyme from the parasite and its host, it was also docked into the available crystal structure of chicken PEPCK (PDB ID 2FAF) and differential binding affinity was observed (R118, K276, C320, R437, D510 and P516). Other two compounds, genistein and PZQ, were predicted to interact with few residues from the nucleotide binding site (online supplementary Table 3), however, daidzein, an analogue of genistein, showed no significant interactions with residues of active site of PEPCK (online supplementary Table 3). THP had the lowest CDocker energy of (−51·3 kcal mol^{-1}) and most numbers of hydrogen bonds with the interacting residues in comparison with other modulators and also to chicken PEPCK docked with the compound. The predicted binding energies (ΔG) showed that every ligand had a negative value, which suggested that all the compounds analysed for binding with PEPCK complexes were likely to be highly stable and that the reactions were spontaneous. The atomic co-ordinates of the possible modulators with PEPCK model (in complex with PEP) of the cestode parasite, *R. echinobothrida*, have been presented in Table 3.

Considering its binding conformations, the propensity of THP to bind to the parasite PEPCK was predicted to be higher than other modulators. In order to find the probable inhibition pattern of THP, top poses of the compound were overlaid with GDP (Fig. 5A) and PEP (Fig. 5B) in the binding site of PEPCK. The docking study predicted that THP bound to the same receptor pocket as GDP, but not in the case of its substrate.

Cloning and purification of recombinant PEPCK and enzyme kinetics

In order to validate the docking simulation results, effect of THP and other modulators on PEPCK

https://doi.org/10.1017/S0031182015001742 Published online by Cambridge University Press

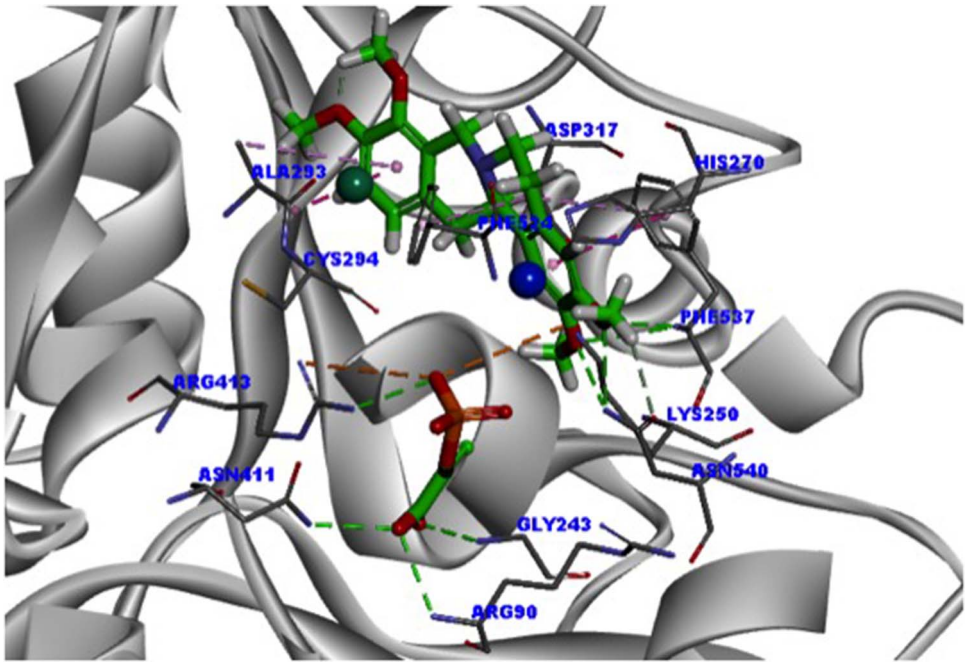

Fig. 4. Likely interactions of THP with the PEPCK model. THP was docked into the active site of PEPCK-PEP-2Mn^{2+} complex using DS 4.1. The protein backbone is rendered as a grey ribbon, and dotted lines represent the hydrogen bonds. The catalytic residues and the ligand are shown as thin and thick stick models, respectively. N atoms are in blue colour, O atoms in red, C atoms in green, and H atoms in grey. Abbreviations: Mn, manganese; PEP, phosphoenolpyruvate; PEPCK, phosphoenolpyruvate carboxykinase; THP, tetrahydropalmatine.

activity was studied. In brief, the ORF of PEPCK was sub-cloned into pE-SUMO vector, and induced by IPTG. The induced recombinant protein was found to be predominantly in the soluble fraction, and then the protein was purified by His6-tag affinity chromatography (on Ni^{2+}-nitrilotriacetate agarose), which gave a band of apparent monomer molecular mass about 70 kDa on SDS-10% (w/v) PAGE (Fig. 6A). As it was a single step purification, few impurities were observed on the SDS-PAGE gel.

Inhibitory constant of THP and other modulators were determined using enzyme kinetics (Table 4). From replots of the slope and *Y*-intercept, it was observed that THP (Fig. 6B–D) and other modulators inhibited PEPCK in a non-competitive manner. Further, it was revealed that THP was more inhibitory than other modulators for PEPCK with *K*i value of 93 nM (Table 4).

Biological relevance of the modulators

Biological significance of the modulators was studied on the parasite *in vitro*. When exposed to defined concentrations of the test compounds, the onset of paralysis ensued in the parasite after ~2–8 h of incubation, while in control the parasites survived up to ~90–96 h (Table 4). After 4 h of exposure, there was a significant decrease in PEPCK activity in the parasite in case of THP (~70%); however, the changes were insignificant for other tested compounds (Table 4). Dosage-dependent experiments revealed a significant decrease in PEPCK activity in the parasite at the concentration of ⩾0·25 mM for THP (Fig. 7A); while time-dependent experiments showed no significant change in the enzyme activity within 1 h of treatment in the case of genistein (data not shown), the activity decreased by ~35% in the case of THP within the same time limit (Fig. 7B).

DISCUSSION

The apparent monomer molecular mass of the parasite PEPCK (~70 kDa), as observed in the present study, is in close agreement with that in other helminths (Klein *et al*. 1992; Liu *et al*. 2006) and also in avian host counterpart (Cook *et al*. 1986). The similarity of PEPCK sequence of the parasite to that of its host, *G. gallus* (cytosolic), and also to *H. sapiens* (cytosolic) is 69 and 56%, respectively. The parasite PEPCK is observed to have higher cysteine content (3·2%), as also in other helminths, in comparison with higher vertebrates and ATP-utilizing PEPCK. However, it is unclear as to why there is high amount of cysteine in helminths compared with others. No disulphide bonds are predicted for PEPCK, even though there are 20 cysteine residues. Likewise, though the native PEPCK (mitochondrial) from chicken contains 13 cysteine residues (Weldon *et al*. 1990), none of these are found to form a disulphide bond (Makinen and Nowak, 1989). The formation of disulphide bonds is suggested to account for not only

https://doi.org/10.1017/S0031182015001742 Published online by Cambridge University Press

Table 3. Atomic co-ordinates of possible modulators with PEPCK model (in complex with PEP) of the cestode parasite, *R. echinobothrida*

Possible modulators	Predicted interacting amino acids	Types of bonds	Distance between the atoms (Å)
THP	A293	Pi sigma/Pi alkyl	5·09
	C294	Pi-hydrophobic	4
	F524	Pi sigma/Pi alkyl	4·86
	F537	Hydrogen bond (N–O19)	3
		Hydrogen bond (N–O21)	3·14
		Pi-hydrophobic	4·45
		Pi sigma/Pi alkyl	5
	N540	Hydrogen bond (N–O19)	2·97
		Hydrogen bond (N–O21)	2·59
		Non classical H-bond (O–H43)	2·91
Genistein	R444	Hydrogen bond (H22–O18)	1·89
	F524	Pi-hydrophobic	5·08
		Pi-hydrophobic	5·4
	F537	Pi-hydrophobic	5·16
		Pi-hydrophobic	4·89
		Pi sigma/Pi alkyl	2·76
PZQ	W523	Pi sigma/Pi alkyl	4·73
		Pi sigma/Pi alkyl	5·25
	F524	Pi sigma/Pi alkyl	3·89
		Pi sigma/Pi alkyl	5·2
	F532	Pi-hydrophobic	4·17
		Pi sigma/Pi alkyl	4·32
	F537	Hydrogen bond (N–O8)	2·94
		Pi-hydrophobic	5·33
		Pi sigma/Pi alkyl	5·48
	N540	Hydrogen bond (N–O8)	3·2
Daidzein	I116	Non classical H-bond (O–H24)	2·17
	Q119	Hydrogen bond (O1–H29)	2·64
		H-bond (H21–O13)	1·97
		Non classical H-bond (H22)	1·86
	R255	Hydrogen bond (H–O19)	2·62
	R491	Pi sigma/Pi alkyl	5·42
	P492	Pi sigma/Pi alkyl	4·48

PEP, phosphoenolpyruvate; PEPCK, phosphoenolpyruvate carboxykinase; PZQ, praziquantel; THP, tetrahydropalmatine.

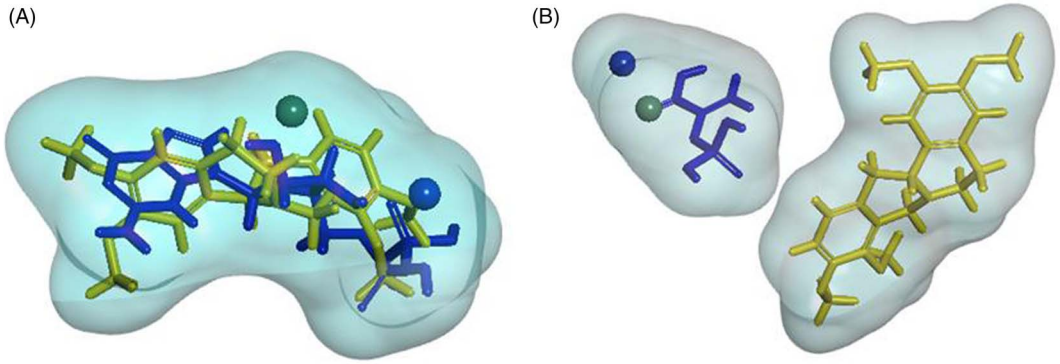

Fig. 5. The molecular overlay of the top poses of THP-GDP-PEPCK complex and THP-PEP-PEPCK complex. DS 4.1 was used to generate a soft surface structure (corresponding to volume of binding site). (A) Surface structure of THP and GDP in the nucleotide binding site (kinase-1 motif) of the enzyme showing similar pocket. (B) Surface structure of THP and PEP showing different binding pockets in the catalytic site of the enzyme. Abbreviations: GDP, guanosine diphosphate; PEP, phosphoenolpyruvate; PEPCK, phosphoenolpyruvate carboxykinase; THP, tetrahydropalmatine.

the loss of free sulfhydryl groups, but also the loss of enzyme activity (Lewis *et al*. 1993; Hlavaty and Nowak, 1997).

The predicted pI of PEPCK is 7·57, indicating the enzyme is active in slightly basic buffers. Sequence analysis using ExPasy-ProtParam tool reveals that

https://doi.org/10.1017/S0031182015001742 Published online by Cambridge University Press

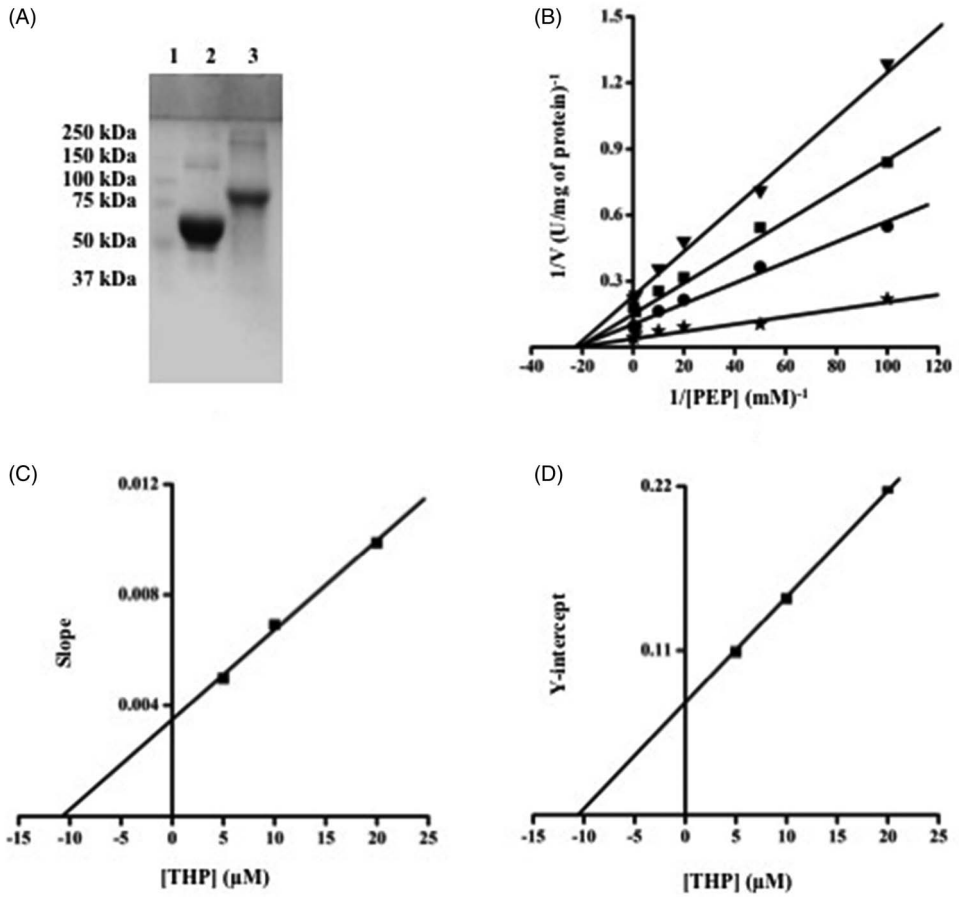

Fig. 6. Purification of recombinant PEPCK and its kinetics. (A) The recombinant PEPCK was induced by IPTG and purified using His6-tag affinity chromatography (on Ni^{2+}-nitrilotriacetate agarose), which gave a band of apparent monomer molecular mass about 70 kDa on SDS-10% (w/v) PAGE: lane 1. molecular weight marker; lane 2. purified digested PEPCK; lane 3. undigested purified PEPCK; (B) Lineweaver–Burk plot showing inhibition of PEPCK activity by THP at variable substrate concentrations. The plot was calculated from assays of seven different concentrations of PEP (0·01 to 8 mM) in the presence of three different concentrations of THP {(*) control, (●) 5 μM, (■) 10 μM, and (▼) 20 μM}; (C) replot of slopes of the lines from the Lineweaver–Burk plot *vs* THP concentration shows positive correlation (R^2 = 0·9964), the intercept on the *X*-axis is $-1/K$i of THP for PEPCK. (D). Replot of *Y*-intercept shows positive correlation ($R^2 = 0·9999$), and the intercept on the *X*-axis is $-1/\alpha K$i of THP for PEPCK. Abbreviations: PEPCK, phosphoenolpyruvate carboxykinase; THP, tetrahydropalmatine.

Table 4. Effect of various modulators (1 mM) on PEPCK activity (U mg^{-1} of protein) and onset of paralysis in *R. echinobothrida in vitro*. Values are expressed as mean ± S.E.M. ($n = 3$).

Modulators	*K*i (μM)[a]	PEPCK activity (U mg^{-1} of protein)	Paralysis time (h)
Control	–	0·263 ± 0·018	~96·0
Vehicle	–	0·234 ± 0·027	~90·0
THP	0·093 ($R^2 = 0·9904$)	0·082 ± 0·009[b]	~4·0
Genistein	0·13 ($R^2 = 0·9964$)	0·210 ± 0·009[c]	~7·0
Daidzein	0·23 ($R^2 = 0·9958$)	0·201 ± 0·017[c]	~8·0
PZQ	0·269 ($R^2 = 0·9996$)	0·213 ± 0·012[c]	~2·0

PEPCK, phosphoenolpyruvate carboxykinase; PZQ, praziquantel; THP, tetrahydropalmatine.
[a] *K*i was determined from Lineweaver–Burk plot as described in the material and methods, and the nature of inhibition was found to be non-competitive for all tested modulators.
[b] Signifies statistical significance in treated parasites compared with control with *P* value of <0·01.
[c] Non significant.

https://doi.org/10.1017/S0031182015001742 Published online by Cambridge University Press

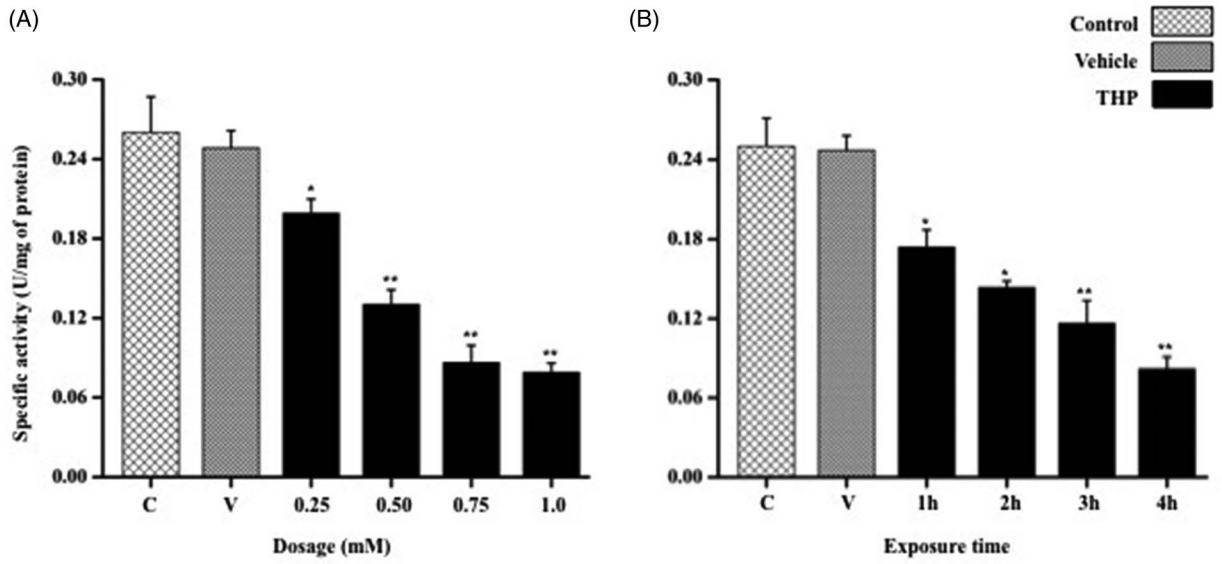

Fig. 7. Dosage- and time-dependent modulatory effect of THP on PEPCK specific activity. *-significant at P value <0·05; **- significant at P value <0·01. (A) Enzyme activity at different dosages of THP at 4 h treatment; (B) enzyme activity at different time intervals in the parasites treated with 1 mM THP. Abbreviations: PEPCK, phosphoenolpyruvate carboxykinase; THP, tetrahydropalmatine.

aliphatic index of PEPCK from the parasite and its host is very high (i.e. 71·91 and 72·09, respectively), indicating that the protein is stable at wide range of temperature as in other PEPCKs (Smith and Caruso, 2013). The instability index of PEPCK is calculated to be 38·95, which provides an estimation of its stability (Guruprasad *et al*. 1990). The GRAVY indices of PEPCK from the parasite and its host are very low (−0·313 and −0·329), as in most other PEPCKs, indicating a high affinity of the enzyme for water or their solubility in hydrophilic solvents (Kyte and Doolittle, 1982). Though, four O-GlcNAc and phosphorylation sites were predicted for the parasite PEPCK (T7, S412,419,470), the enzyme is unlikely to be regulated either by glycosylation or phosphorylation (Yang *et al*. 2009).

In the absence of information on crystal structures, homology models are often valuable for rationalizing existing evidence and guiding new experiments (Baker and Sali, 2001). PEPCK homology models have been prepared for various organisms, e.g. *Anaerobiospirillum succiniciproducens* (Jabalquinto *et al*. 2002), *Saccharomyces cerevisiae* (Villarreal *et al*. 2006), *A. suum* (Verma *et al*. 2012), *S. mansoni* (Swargiary *et al*. 2013), and Cyanobacteria (Smith and Caruso, 2013). In the present study, a homology model was prepared using the crystal structure of rat cytosolic PEPCK as template, and this shows a sequence identity of 54·5% containing all the active sites and catalytic domains of the protein. The active sites of the modelled PEPCK are also found in the chicken mitochondrial PEPCK containing all mobile elements and motifs, with slight variations in the residue positions. Structural studies on PEPCK from various organisms show that the catalytic sites are well conserved (Hanson, 2009). In general, the active site of the enzyme lies in a deep extended groove between the N- and C- terminal domains, whereas cationic residues like arginine, lysine and histidine play an important role in substrate binding and catalysis (Cheng and Nowak, 1989; Matte *et al*. 1997). The active site of the enzyme also contains the 15-residue mobile Ω -loop lid domain (^{470}SEATAAAEFKGRQVM^{484} in this study), the closure of which is critical for catalysis. The R-loop is another mobile element (^{88}VARVESKT^{95} in PEPCK from the parasite) that contains the catalytically active arginine residue (R90) for substrate binding (Carlson and Holyoak, 2009). The nucleotide binding site (kinase 1 motif) and metal ion binding site (kinase 2) are the conserved catalytic domains of the protein belonging to kinase family. In most species of PEPCK, there are about 10–15 amino acids separating the kinase 1 and 2 motifs (Cheek *et al*. 2002). Analysis of the enzyme from both the parasite and its host shows that there are 15 residues between these motifs. The enzyme also contains the reactive cysteine residue (C294) at its P-loop domain that is conserved in all GTP-dependent PEPCKs (Lewis *et al*. 1989; Makinen and Nowak, 1989). It is reported that the metal binding site of PEPCK from *G. gallus* gets cleaved in the presence of ascorbate, an observation that has been subsequently confirmed in *A. suum* PEPCK as well (Hlavaty and Nowak, 1997). This observation suggests a close similarity of the catalytic site in helminth parasites and higher vertebrates.

https://doi.org/10.1017/S0031182015001742 Published online by Cambridge University Press

Docking against homology-modelled structures is used to understand structure-activity relationships (Marhefka *et al*. 2001). Docking scores are essentially approximations to the true binding constant, which are based mostly on the non-covalent interactions between the ligand and the target (Huang *et al*. 2010). Atomic coordination of the metal ion (M1) was found to directly co-ordinate with K250, H270 and D317 residues of PEPCK model as observed in other crystal structures (PDB IDs 4GNP, 4GMW, 2FAH, and 2QZY). The substrate and co-factors, when docked with the PEPCK model, resulted in similar interactions comparable with the available corresponding crystal complexes. The arginine residue of the mobile R-loop, which binds directly to the PEP through electrostatic interactions (Johnson and Holyoak, 2012) as shown in the crystal structure of chicken mitochondrial PEPCK (PDB ID 2QZY) is also observed in our docking study (R90) corresponding to R87 in the template structure. A comparison of GDP docked complex, in the present study, with the GDP-bound chicken mitochondrial PEPCK (PDB ID 2FAH) shows conservation of P-loop residues. Although the active site residues are conserved in PEPCK from the parasite and its host, conformational sampling and structural fluctuations may contribute towards differential binding of the ligands. It has been shown that ligand binding depends on the microenvironment of the enzyme active sites, and conformational dynamics of the protein, which play an important role in binding event (Hammes, 2002).

The docking studies are performed considering several parameters of the selected ligands, such as molecular weight, number of rotatable bonds, hydrogen bond and the donor and acceptor groups (Lipinski *et al*. 2001). In the present study, molecular docking of all the tested modulators predicted that THP, genistein and PZQ interacted with active site residues of PEPCK from the parasite, whereas daidzein did not show any interaction with any active site residue. THP was predicted to interact with residues of the nucleotide binding site; it inhibited the recombinant PEPCK in a non-competitive manner for its substrate, which was also predicted in our molecular docking study (Fig. 5B). It was found to have lowest *K*i, more significantly compared with other compounds as corroborated by *in vitro* study. Hence, THP may be predicted as a potential GDP inhibitor in the enzyme catalysis. However, it would be possible to pin point the exact mechanism of inhibition of PEPCK by THP only when ligand-bound crystal structures are available. It may be hypothesized that the enzyme selectively inhibits and provides a target for anthelmintic action because of difference of its primary function between cestodes and their vertebrate hosts (Reynolds, 1980). Inhibition of the enzyme activity resulting in retarded glucose oxidation may, in turn, cause subsequent paralysis in the parasite. However, in the case of PZQ, which primarily acts upon voltage-operated Ca^{2+} channels (Chan *et al*. 2013), no change in PEPCK activity was observed. In contrast, mebendazole, a broad spectrum anthelmintic, disrupts certain enzymes of carbohydrate metabolism, which may ultimately cause death of cestodes (Ahmad and Nizami, 1987).

In conclusion, in the present study, we could deduce the complete CDS of PEPCK from *R. echinobothrida*. Results from our computational studies reveal that the parasite PEPCK is structurally similar to that of its avian host and that THP may be used as an inhibitor for the enzyme. Further, crystallographic studies would help to understand the molecular interactions of THP with PEPCK.

SUPPLEMENTARY MATERIAL

To view supplementary material for this article, please visit http://dx.doi.org/10.1017/S0031182015001742

ACKNOWLEDGEMENTS

We thank Dr. Todd Holyoak, University of Waterloo, Canada, for providing pE-SUMO vector and pE-SUMO protease for expression studies. Thanks are due to the Head, Department of Zoology, NEHU, for providing infrastructural facilities for the work.

FINANCIAL SUPPORT

This work was supported by Department of Biotechnology (Government of India), New Delhi, through a research project sanctioned to B. D., V. T. and A. S. (sanction no. BT/PR 12828/Med/30/221/2009, dated March 22, 2010).

REFERENCES

Ahmad, M. and Nizami, W. A. (1987). *In vitro* effects of mebendazole on the carbohydrate metabolism of *Avitellina lahorea* (Cestoda). *Journal of Helminthology* **61**, 247–252.

Baker, D. and Sali, A. (2001). Protein structure prediction and structural genomics. *Science* **294**, 93–96.

Bradford, M. M. (1976). A rapid and sensitive method for the quantification of microgram quantities of protein utilizing the principle of protein dye binding. *Analytical Biochemistry* **72**, 248–254.

Carlson, G. M. and Holyoak, T. (2009). Structural insights into the mechanism of phosphoenolpyruvate carboxykinase catalysis. *Journal of Biological Chemistry* **284**, 27037–27041.

Chan, J. D., Zarowiecki, M. and Marchant, J. S. (2013). Ca^{2+} channels and Praziquantel: a view from the free world. *Parasitology International* **62**, 619–628.

Cheek, S., Zhang, H. and Grishin, N. V. (2002). Sequence and classification of kinases. *Journal of Molecular Biology* **320**, 855–881.

Cheng, K. C. and Nowak, T. (1989). Arginine residues at the active site of avian liver phosphoenolpyruvate carboxykinase. *Journal of Biological Chemistry* **264**, 3317–3324.

Cook, J. S., Weldon, S. L., Garcia-Ruiz, J. P., Hod, Y. and Hanson, R. W. (1986). Nucleotide sequence of the mRNA encoding the cytosolic form of phosphoenolpyruvate carboxykinase (GTP) from the chicken. *Proceedings of the National Academy of Sciences of USA* **83**, 7583–7587.

Das, B., Tandon, V. and Saha, N. (2004). Effects of phytochemicals of *Flemingia vestita* (Fabaceae) on glucose 6-phosphate dehydrogenase and enzymes of gluconeogenesis in a cestode (*Raillietina echinobothrida*). *Comparative Biochemistry and Physiology – Part C* **139**, 141–146.

Das, B., Tandon, V., Saxena, J. K., Joshi, S. and Singh, A. R. (2013). Purification and characterization of phosphoenolpyruvate carboxykinase from *Raillietina echinobothrida*, a cestode parasite of the domestic fowl. *Parasitology* **140**, 136–146.

Ghedin, E., Wang, S., Spiro, D., Caler, E., Zhao, Q., Crabtree, J., Allen, J. E., Delcher, A. L., Guiliano, D. B., Miranda-Saavedra, D., Angiuoli, S. V., Creasy, T., Amedeo, P., Haas, B., El-Sayed, N. M., Wortman, J. R., Feldblyum, T., Tallon, L., Schatz, M., Shumway, M., Koo, H., Salzberg, S. L., Schobel, S., Pertea, M., Pop, M., White, O., Barton, G. J., Carlow, C. K., Crawford, M. J., Daub, J., Dimmic, M. W., Estes, C. F., Foster, J. M., Ganatra, M., Gregory, W. F., Johnson, N. M., Jin, J., Komuniecki, R., Korf, I., Kumar, S., Laney, S., Li, B. W., Li, W., Lindblom, T. H., Lustigman, S., Ma, D., Maina, C. V., Martin, D. M., McCarter, J. P., McReynolds, L., Mitreva, M., Nutman, T. B., Parkinson, J., Peregrín-Alvarez, J. M., Poole, C., Ren, Q., Saunders, L., Sluder, A. E., Smith, K., Stanke, M., Unnasch, T. R., Ware, J., Wei, A. D., Weil, G., Williams, D. J., Zhang, Y., Williams, S. A., Fraser-Liggett, C., Slatko, B., Blaxter, M. L. and Scott, A. L. (2007). Draft genome of the filarial nematode parasite *Brugia malayi*. *Science* **317**, 1756–1760.

Guruprasad, K., Reddy, B. V. B. and Pandit, M. W. (1990). Correlation between stability of a protein and its dipeptide composition: a novel approach for predicting *in vivo* stability of a protein from its primary sequence. *Protein Engineering* **4**, 155–161.

Hammes, G. G. (2002). Multiple conformational changes in enzyme catalysis. *Biochemistry* **41**, 8221–8228.

Hanson, R. W. (2009). Thematic minireview series: a perspective on the biology of phosphoenolpyruvate carboxykinase 55 years after its discovery. *Journal of Biological Chemistry* **284**, 27021–27023.

Hlavaty, J. J. and Nowak, T. (1997). Affinity cleavage at the metal-binding site of phosphoenolpyruvate carboxykinase. *Biochemistry* **36**, 15514–15525.

Holyoak, T., Sullivan, S. M. and Nowak, T. (2006). Structural insights into the mechanism of PEPCK catalysis. *Biochemistry* **45**, 8254–8263.

Huang, S. Y., Grinter, S. Z. and Zou, X. (2010). Scoring functions and their evaluation methods for protein-ligand docking: recent advances and future directions. *Physical Chemistry Chemical Physics* **12**, 12899–12908.

Jabalquinto, A. M., Laivenieks, M., González-Nilo, F. D., Yévenes, A., Encinas, M. V., Zeikus, J. G. and Cardemil, E. (2002). Evaluation by site-directed mutagenesis of active site amino acid residues of *Anaerobiospirillum succiniciproducens* phosphoenolpyruvate carboxykinase. *Journal of Protein Chemistry* **21**, 393–400.

Jo, J. S., Ishihara, N. and Kikuchi, G. (1974). Occurrence and properties of four forms of phosphoenolpyruvate carboxykinase in the chicken liver. *Archives of Biochemistry and Biophysics* **160**, 246–254.

Johnson, T. A. and Holyoak, T. (2012). The Ω-loop lid domain of phosphoenolpyruvate carboxykinase is essential for catalytic function. *Biochemistry* **51**, 9547–9559.

Klein, R. D., Winterrowd, C. A., Hatzenbuhler, N. T., Shea, M. H., Favreau, M. A., Nulf, S. C. and Geary, T. G. (1992). Cloning of a cDNA encoding phosphoenolpyruvate carboxykinase from *Haemonchus contortus*. *Molecular and Biochemical Parasitology* **50**, 285–294.

Knapp, J., Nakao, M., Yanagida, T., Okamoto, M., Saarma, U., Lavikainen, A. and Ito, A. (2011). Phylogenetic relationships within *Echinococcus* and *Taenia* tapeworms (Cestoda: Taeniidae): an inference from nuclear protein-coding genes. *Molecular Phylogenetics and Evolution* **61**, 628–638.

Kyte, J. and Doolittle, R. F. (1982). A simple method for displaying the hydropathic character of a protein. *Journal of Molecular Biology* **157**, 105–132.

Lewis, C. T., Haley, B. E. and Carlson, G. M. (1989). Formation of an intramolecular cystine disulfide during the reaction of 8-azidoguanosine 5′-triphosphate with cytosolic phosphoenolpyruvate carboxykinase (GTP) causes inactivation without photolabeling. *Biochemistry* **28**, 9248–9255.

Lewis, C. T., Seyer, J. M., Cassell, R. G. and Carlson, G. M. (1993). Identification of vicinal thiols of phosphoenolpyruvate carboxykinase (GTP). *Journal of Biological Chemistry* **268**, 1628–1636.

Lipinski, C. A., Lombardo, F., Dominy, B. W. and Feeney, P. J. (2001). Experimental and computational approaches to estimate solubility and permeability in drug discovery and development settings. *Advanced Drug Delivery Reviews* **46**, 3–26.

Liu, F., Lu, J., Hu, W., Wang, S. Y., Cui, S. J., Chi, M., Yan, Q., Wang, X. R., Song, H. D., Xu, X. N., Wang, J. J., Zhang, X. L., Zhang, X., Wang, Z. Q., Xue, C. L., Brindley, P. J., McManus, D. P., Yang, P. Y., Feng, Z., Chen, Z. and Han, Z. G. (2006). New perspectives on host-parasite interplay by comparative transcriptomic and proteomic analyses of *Schistosoma japonicum*. *PLoS Pathogens* **2**, e29.

Makinen, A. L. and Nowak, T. (1989). A reactive cysteine in avian liver phosphoenolpyruvate carboxykinase. *Journal of Biological Chemistry* **264**, 12148–12157.

Marhefka, C. A., Moore, B. M., Bishop, T. C., Kirkovsky, L., Mukherjee, A., Dalton, J. T. and Miller, D. D. (2001). Homology modeling using multiple molecular dynamics simulations and docking studies of the human androgen receptor ligand binding domain bound to testosterone and nonsteroidal ligands. *Journal of Medicinal Chemistry* **44**, 1729–1740.

Matte, A., Tari, L. W., Goldie, H. and Delbaere, L. T. J. (1997). Structure and mechanism of phosphoenolpyruvate carboxykinase. *Journal of Biological Chemistry* **272**, 8105–8108.

Mommsen, T. P., Patrick, J. W. and Moon, T. W. (1985). Gluconeogenesis in hepatocytes and kidney of Atlantic salmon. *Molecular Physiology* **8**, 89–100.

Reynolds, C. H. (1980). Phosphoenolpyruvate carboxykinase from the rat and from the tapeworm, *Hymenolepis diminuta*. *Comparative Biochemistry and Physiology* **65**, 481–487.

Ríos, S. E. and Nowak, T. (2002). Role of cysteine 306 in the catalytic mechanism of *Ascaris suum* phosphoenolpyruvate carboxykinase. *Archives of Biochemistry and Biophysics* **404**, 25–37.

Rollinger, J. M., Stuppner, H. and Langer, T. (2008). Virtual screening for the discovery of bioactive natural products. *Progress in Drug Research* **65**, 213–249.

Smith, A. A. and Caruso, A. (2013). *In silico* characterization and homology modeling of a cyanobacterial phosphoenolpyruvate carboxykinase enzyme. *Structural Biology*, Article ID 370820, 10.

Smyth, J. D. and McManus, D. P. (1989). *The Physiology and Biochemistry of Cestodes*. Cambridge University Press, Cambridge, UK.

Soulsby, E. J. L. (1982). *Helminths, Arthropods and Protozoa of Domesticated Animals*, 7th Edn, ELBS and Bailliere Tindall, London.

Swargiary, A., Verma, A. K. and Sarma, K. (2013). Homology modeling and docking studies of phosphoenolpyruvate carboxykinase in *Schistosoma mansoni*. *Medicinal Chemistry Research* **22**, 2870–2878.

Tandon, V. and Das, B. (2007). *In vitro* testing of anthelmintic efficacy of *Flemingia vestita* (Fabaceae) on carbohydrate metabolism in *Raillietina echinobothrida*. *Methods* **42**, 330–338.

Utter, M. F. and Kurahashi, K. (1954). Purification of oxalacetic carboxylase from chicken liver. *Journal of Biological Chemistry* **207**, 787–802.

Verma, A. K., Swargiary, A., Prasad, S. B. and Arjun, J. (2012). Homology modeling of phosphoenolpyruvate carboxykinase of *Ascaris suum*. *Journal of Pharmacy Research* **5**, 1248–1255.

Villarreal, J. M., Bueno, C., Arenas, F., Jabalquinto, A. M., González-Nilo, F. D., Encinas, M. V. and Cardemil, E. (2006). Nucleotide specificity of *Saccharomyces cerevisiae* phosphoenolpyruvate carboxykinase kinetics, fluorescence spectroscopy, and molecular simulation studies. *International Journal of Biochemistry and Cell Biology* **38**, 576–588.

Wang, X., Chen, W., Huang, Y., Sun, J., Men, J., Liu, H., Luo, F., Guo, L., Lv, X., Deng, C., Zhou, C., Fan, Y., Li, X., Huang, L., Hu, Y., Liang, C., Hu, X., Xu, J. and Yu, X. (2011). The draft genome of the carcinogenic human liver fluke *Clonorchis sinensis*. *Genome Biology* **12**, R107.

Weldon, S. L., Rando, A., Matathias, A. S., Hod, Y., Kalonick, P. A., Savon, S., Cook, J. S. and Hanson, R. W. (1990). Mitochondrial phosphoenolpyruvate carboxykinase from the chicken. Comparison of the cDNA and protein sequences with the cytosolic isozyme. *Journal of Biological Chemistry* **265**, 7308–7317.

Yang, J., Kalhan, S. C. and Hanson, R. W. (2009). What is the metabolic role of phosphoenolpyruvate carboxykinase? *Journal of Biological Chemistry* **284**, 27025–27029.